



OPEN ACCESS

RECEIVED

2 September 2019

REVISED

4 January 2020

ACCEPTED FOR PUBLICATION

13 January 2020

PUBLISHED

23 January 2020

Original content from this work may be used under the terms of the [Creative Commons Attribution 3.0 licence](#).

Any further distribution of this work must maintain attribution to the author(s) and the title of the work, journal citation and DOI.



PAPER

Schemes for nondestructive quantum gas microscopy of single atoms in an optical lattice

Daichi Okuno¹, Yoshiki Amano¹, Katsunari Enomoto² , Nobuyuki Takei¹ and Yoshiro Takahashi¹¹ Department of Physics, Graduate School of Science, Kyoto University, 606-8502, Japan² Department of Physics, University of Toyama, 930-8555, JapanE-mail: okuno.daichi@yagura.scphys.kyoto-u.ac.jp**Keywords:** quantum non-demolition measurement, quantum gas microscope, squeezed vacuum

Abstract

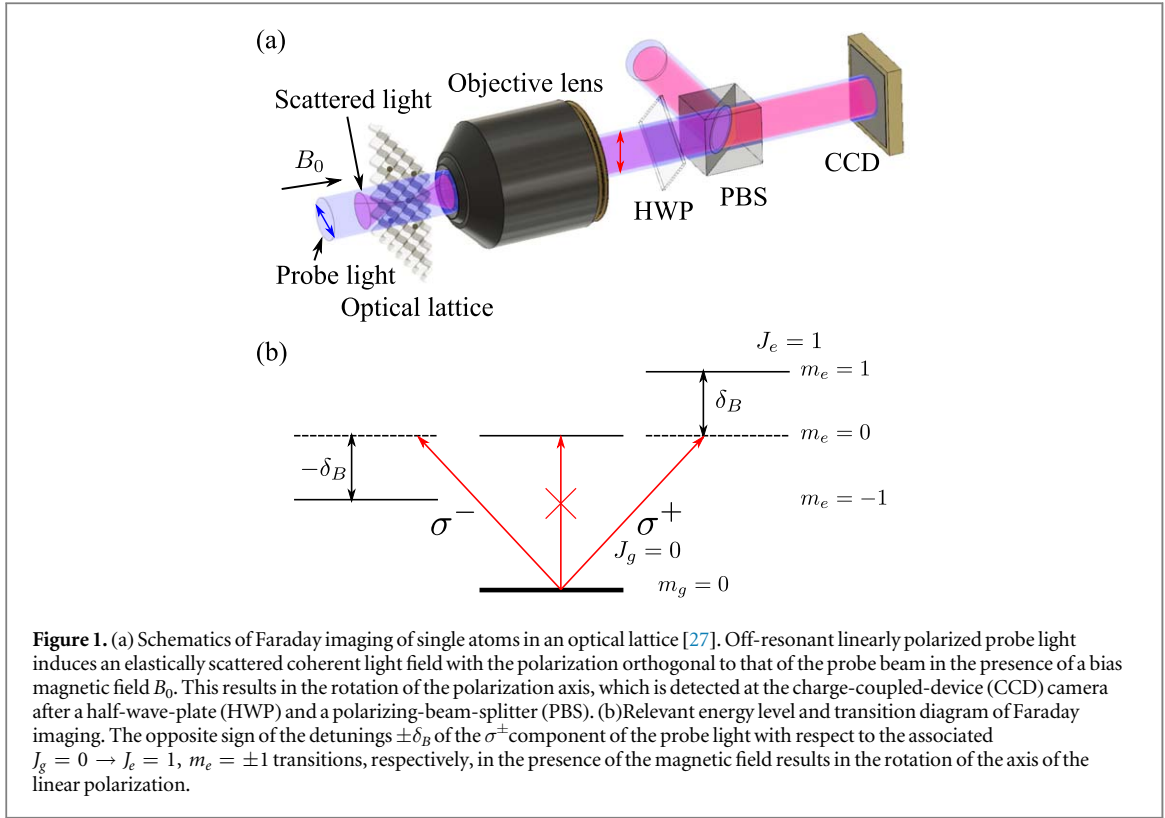
We propose a quantum gas microscope for ultracold atoms that enables nondestructive atom detection, thus evading higher-band excitation and change of the internal degrees of freedom. We show that photon absorption of a probe beam cannot be ignored even in dispersive detection to obtain a signal-to-noise ratio greater than unity because of the shot noise of the probe beam under a standard measurement condition. The first scheme we consider for the nondestructive detection, applicable to an atom that has an electronic ground state without spin degrees of freedom, is to utilize a magic-wavelength condition of the optical lattice for the transition for probing. The second is based on the dispersive Faraday effect and squeezed quantum noise and is applicable to an atom with spins in the ground state. In this second scheme, a scanning microscope is adopted to exploit the squeezed state and reduce the effective losses. Application to ultracold ytterbium atoms is discussed.

1. Introduction

A quantum gas microscope for ultracold atoms is a powerful tool to study the dynamics and properties of quantum gases in one- or two-dimensional optical lattices [1–7]. It directly monitors many lattice sites with single-site resolution. It is also possible to deterministically prepare nearly arbitrary initial states by performing single-site control on an atomic Mott-insulator state [8]. This versatile technique has promoted many fascinating studies [9] such as quantum random walks [8, 10], direct observation of antiferromagnetic spin correlation [11–13], and measuring entanglement entropy in a quantum many-body system [14].

In the quantum gas microscopy, the number of atoms in each lattice site, more precisely the parity of the number of atoms, is measured by detecting photons spontaneously emitted from the atoms after freezing the hopping by suddenly increasing the optical lattice potential. This measurement process induces considerable recoil heating, requiring an elaborate cooling scheme in a deep optical lattice. Even with the cooling of the atoms in an optical lattice site, the imaging fidelity is not perfect [4–6]. In the present work, we only consider nondestructive measurement schemes which do not rely on any cooling procedure.

If one can nondestructively measure the number of atoms with avoidance of the higher-band excitations, one can study the subsequent quantum many-body dynamics starting from the product state of the fixed numbers of atoms as a result of the atom-number projective measurement. Here we use the term ‘nondestructive’ in the measurement of an observable of interest \hat{A} such as a spin or an atom number in the sense that the probability distributions P_a of measurement outcome a of \hat{A} are the same before and after the measurement [15]. An example of interesting quantum many-body dynamics is the quantum critical behavior of the Bose–Hubbard systems influenced by measurement backaction [16] and the creation of a strong correlation with feedback control [17]. From a technical viewpoint, realization of the nondestructive limit of quantum gas microscopy relaxes the crucial requirement of incorporating an elaborate cooling scheme for an extremely deep optical lattice depth. We note that nondestructive monitoring of quantum dynamics of cold atoms in a cavity quantum electrodynamics setup using a scanning microscope is recently proposed [18, 19].



One may expect that the dispersive method using off-resonant probe light such as a Faraday effect can detect atoms without photon absorption by taking a sufficiently large detuning. However, it has been discussed that both measurements using resonant and off-resonant light have the same sensitivity for an optically thin sample for a given extent of absorption [20–22]. This is because of the existence of the shot noise in the probe light in the interferometric measurement of the dispersive method. Thus far, there is no quantitative discussion regarding the detection limit of a single atom under the condition of quantum gas microscopy in which the light can be efficiently collected by an objective lens with a high numerical aperture A_N .

In this paper, first we discuss the limitation of quantum gas microscopy with a dispersive Faraday effect. We show that the photon absorption of the probe beam cannot be ignored to obtain a signal-to-noise ratio R_{SN} greater than unity even under an ideal condition of $A_N = 1$, which is reminiscent of the result for an optically thin sample [20–22].

To overcome this limitation, we propose two schemes. The first is to utilize the magic-wavelength condition of the optical lattice for the transition of probing. The tight confinement in a Lamb–Dicke regime provides optical transitions mostly between states with the same vibrational quantum number in the optical lattice sites, thus satisfying the ‘nondestructive’ condition. This is only applicable for atoms in the ground state without any spin degrees of freedom, such as a bosonic isotope of two-electron atoms. The second is a scanning-type quantum gas microscope with a confocal configuration with the use of a broadband squeezed vacuum [23–26]. Utilizing the squeezed vacuum and heterodyne detection of scattered light from the atoms during the Faraday process in quantum gas microscopy, we achieve an R_{SN} greater than one while suppressing the light absorption and associated higher-band excitations. A scanning microscope with a confocal configuration is necessary to avoid effective losses on the squeezed state because of the branching of the spatial distribution of the light and mode-mismatch between the squeezed light and a local oscillator (LO) in the heterodyne detection. We discuss a system of two-electron atoms in metastable states as a realistic example of the application of the proposed scheme, enabling spin-sensitive nondestructive observation of a $SU(N)$ Fermi–Hubbard model.

2. Limitation of dispersive QGM

Before going to our proposal schemes for nondestructive imaging, we discuss the limitation of quantum gas microscopy with a dispersive Faraday interaction. Figure 1(a) shows the schematic setup [27]. We assume the transition $J_g = 0 \rightarrow J_e = 1$ for probing the atoms for simplicity, as shown in figure 1(b). When we set the frequency of the probe beam at the center of the $J_g = 0 \rightarrow J_e = 1, m_e = \pm 1$ transitions in the presence of a bias magnetic field B_0 applied along the probe propagation axis, the σ^+ and σ^- circular polarization components of

the linearly polarized probe beam have different detunings $\pm\delta_B$ provided by the magnetic field. This causes different phase shifts in the two components and therefore induces the rotation of the axis of linear polarization of the probe beam, termed the Faraday effect. The polarization rotation signal for a single atom can be understood as an effect of interference between a linearly polarized input probe beam $\vec{E}_{\text{probe}}(r)$ and an elastically scattered electric field coherently induced by a single atom. Based on diffraction theory [28] and scattering theory [29], the scattered light field $\vec{E}_{\text{sc}}(r)$ is described [27] as

$$\vec{E}_{\text{sc}}(r) = \alpha \frac{2J_1(r/\sigma)}{r/\sigma} E_0 \left(\frac{\hat{e}_+}{1 - i(2\delta_B/\Gamma)} + \frac{\hat{e}_-}{1 + i(2\delta_B/\Gamma)} \right), \quad (1)$$

where Γ is the natural linewidth of the excited state. E_0 is the amplitude of the electric field of the input probe beam, $\alpha = -\sqrt{3}\eta A_N/2$, where $\eta \equiv [1 - (1 - A_N^2)^{1/2}(1 - A_N^2/4)]/2$ is the photon collection efficiency of an objective lens, $J_1(x)$ is the Bessel function of the first kind, $\sigma \equiv (kA_N)^{-1}$ is the diffraction-limited spatial resolution, k is the wavenumber of the probe light, and \hat{e}_{\pm} is the polarization unit vector for σ^{\pm} circularly polarized light. For large δ_B/Γ , the scattered light polarization is perpendicular to the initial polarization of the probe light and has the expected $1/\delta_B$ dependence.

Under this condition, we can derive the expression for R_{SN} as follows:

$$R_{\text{SN}} = \sqrt{\frac{\epsilon_0 c}{2}} \frac{\int_{\text{det}} dA \vec{E}_{\text{sc}} \cdot \vec{E}_{\text{probe}}}{\sqrt{\int_{\text{det}} dA |\vec{E}_{\text{probe}}|^2}} \sqrt{\frac{\lambda \tau}{hc}}. \quad (2)$$

Here the signal is the difference in the intensities of the two detected fields $\vec{E}_{\text{detect}}(r)_{\pm} = \frac{1}{\sqrt{2}}(\vec{E}_{\text{probe}}(r) \pm \vec{E}_{\text{sc}}(r))$, and the noise is the shot-noise given as follows:

$$N = \sqrt{\int_{\text{det}} \left(\frac{\epsilon_0 c}{2} \right) |\vec{E}_{\text{probe}}|^2 dA \frac{\lambda \tau}{hc}} \quad (3)$$

(see [appendix](#)). The integral area is the domain over the detector. The parameter τ represents the temporal width of the probe pulse. ϵ_0 , c , h and λ are the permittivity of vacuum, the speed of light, the Planck constant, and the wavelength of the transition, respectively. For a large δ_B/Γ , R_{SN} becomes

$$R_{\text{SN}} = \sqrt{\frac{\Gamma \tau}{2}} s \eta C_{\text{sc,probe}}, \quad (4)$$

where

$$C_{\text{sc,probe}} = \int_{\text{det}} \vec{E}_{\text{sc}} \cdot \vec{E}_{\text{probe}} dA / \sqrt{\int_{\text{det}} |\vec{E}_{\text{sc}}|^2 dA} \sqrt{\int_{\text{det}} |\vec{E}_{\text{probe}}|^2 dA} \quad (5)$$

is the quantity representing the level of the spatial mode-matching between the probe beam $\vec{E}_{\text{probe}}(r)$ and the scattered light $\vec{E}_{\text{sc}}(r)$, and

$$s = \frac{I_0/I_{\text{sat}}}{1 + (2\delta_B/\Gamma)^2} \simeq \frac{I_0/I_{\text{sat}}}{(2\delta_B/\Gamma)^2} \quad (\delta_B \gg \Gamma) \quad (6)$$

is the saturation parameter with a saturation intensity $I_{\text{sat}} = \pi \hbar c \Gamma / (3 \lambda^3)$ and the probe intensity $I_0 = \frac{\epsilon_0 c}{2} |E_0|^2$. The number of photon absorption N_{abs} is given for a large δ_B/Γ as follows:

$$N_{\text{abs}} = \frac{\Gamma \tau}{2} s. \quad (7)$$

From equations (4) and (7), we obtain the important following relation:

$$N_{\text{abs}} = R_{\text{SN}}^2 / (\eta C_{\text{sc,probe}}^2). \quad (8)$$

The maximum values of η and $C_{\text{sc,probe}}$ are $1/2$ for $A_N = 1$ and 1 for $E_{\text{probe}}(r) = E_{\text{sc}}(r)$ with a sufficiently large integration area, respectively. Note that this high level of mode matching is achieved only for a particular single site. If we consider the probe beam sufficiently broad compared to the lattice constant, $C_{\text{sc,probe}} = 0.85$ for the optimal integration area can be derived by a simple calculation. From these considerations, we conclude that the number of photon absorptions of the probe beam is never less than 1 at $R_{\text{SN}} = 1$. Under the more realistic condition of $A_N = 0.8$ ($\eta = 0.248$) and the Gaussian spatial mode of the probe beam with an optimal waist, where $C_{\text{sc,probe}}$ becomes 0.91 , the minimum number of photon absorptions is 4.8 at $R_{\text{SN}} = 1$.

3. Proposed schemes

We consider the two strategies to overcome this fundamental limitation. The first, applicable to an atom that has an electronic ground state without spin degrees of freedom, is to utilize tight confinement of the atom under a

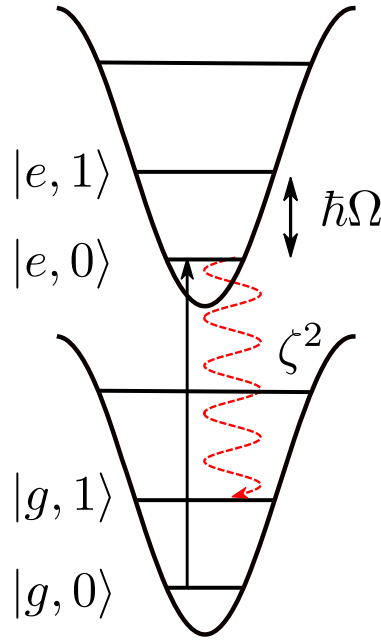
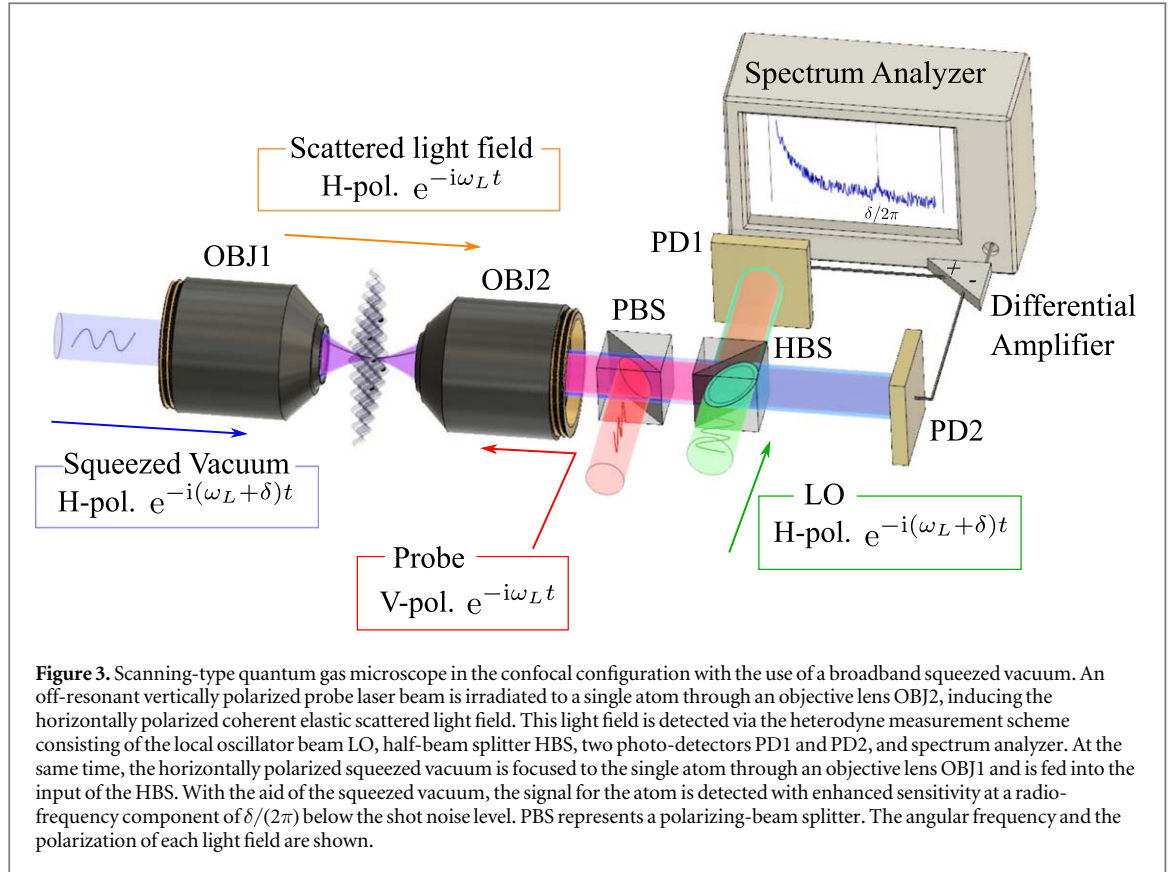


Figure 2. Vibrational level structure of an atom tightly confined in an optical lattice with a magic-wavelength condition ($\Omega_e = \Omega_g = \Omega$) for the transition for probing. During the absorption process, the probe laser beam whose linewidth is much narrower than the trap frequency Ω is tuned to the well-resolved resonance of the $|g, 0\rangle \rightarrow |e, 0\rangle$ transition. During the spontaneous emission process, the transition predominantly occurs between the vibrational ground states in the electronic ground $|g, 0\rangle$ and excited $|e, 0\rangle$ states, and the transition accompanying the change in one vibrational quantum number $|e, 0\rangle \rightarrow |g, 1\rangle$ is suppressed by the square of the Lamb–Dicke factor ζ compared to the transition $|e, 0\rangle \rightarrow |g, 0\rangle$.

magic-wavelength condition of the optical lattice for the transition for probing (see figure 2). In general, vibrational quantum number can change without any preference during the probe transition. If we irradiate the probe light to the atom tightly confined in the optical lattice site in three dimensions formed by the magic-wavelength light of the probe transition, the probe photon absorption and subsequent spontaneous emission process predominantly occur between the vibrational ground states in the electronic ground and excited states (carrier), and the transition accompanying the change in one vibrational quantum number (sideband) is suppressed by the square of the Lamb–Dicke factor $\zeta = \sqrt{\omega_R/\Omega}$ compared to the transition between the same vibrational quantum numbers [30]. Here $\hbar\omega_R = \hbar^2 k_{\text{lat}}^2/2m$ is the recoil energy of the lattice and Ω is the trapping frequency. Here k_{lat} is the wavenumber of the lattice laser and m is the atom mass. For simplicity, we consider the case where the trapping frequencies are the same for all three directions, and Γ and the linewidth of the probe light $\Delta\nu_{\text{probe}}$ are sufficiently narrow such that the probe laser is solely resonant to the carrier transition, which is well-resolved from the sideband transitions: $\Gamma, \Delta\nu_{\text{probe}} \ll \Omega$. Then, we can repeat the photon absorption and subsequent spontaneous emission between the vibrational ground states before $N_{\text{abs}} \times 3\zeta^2$ reaches one, and therefore the criterion for ‘nondestructive’ relaxes as $N_{\text{abs}} < 1/(3\zeta^2)$. We note this scheme does not require cooling procedure during the imaging, such as Raman sideband cooling. While the fidelities of the atom detection with some cooling methods could be now even higher than those in the first demonstrations [4–6], in our work, however, we specifically discuss more stringent probing condition in which the vibrational state of an atom in each lattice site minimally changes. Regarding ytterbium (Yb) atoms, the realization of Lamb–Dicke confinement with $\zeta = 0.11$ in the ‘magic-like’ lattice for the $^1S_0 - ^3P_1$ transition is already demonstrated using the 532 nm laser light with an appropriate polarization choice [31].

However, in general cases of atoms with spins in the ground state, the situation is not so simple. It is true that, in a magic-wavelength lattice, we can think of a scheme of spin-preserving probing such as a closed, cyclic transition with appropriate polarization of probe light, or spin-non-preserving probing of one particular spin-component, say spin-up, and later performing optical pumping to the original spin-up state with shelving another spin-component, say spin-down, to states irrelevant for probing, and finally returning the atom to their original spin-down state. However, here we think of a much simpler scheme where no additional processes that influence the performance of the nondestructive detection are required other than probing. If the detection without photon absorption is possible, it is ideal for realizing nondestructive detection. For this purpose, we propose the second scheme of a scanning-type quantum gas microscope in the confocal configuration with the use of a broadband squeezed vacuum. An imaging system we consider is shown in figure 3. Squeezed light has been used to reduce the shot noise [23]. It has been considered to be incorporated into a gravitational wave detector to beat the standard quantum limit [32]. It has also been shown to be an important resource of



spectroscopy [26], biological measurement [33], magnetometry [24, 25], and continuous-variable quantum information processing [34]. Note that a squeezed vacuum is fragile to branching. Array detectors such as CCD cameras are not compatible with squeezed light because imaging with array detectors involves light branching to each detector segment. Therefore, measurement should be completed for each site with a single balanced detection mode scanning one-by-one as shown in figure 3. Mode-matching and scanning with the single site addressing level can be accomplished by a digital micromirror device and a galvano mirror system, for example.

The target lattice site is selectively illuminated by an off-resonant weak probe laser beam with an angular frequency ω_L and vertical linear polarization through an objective lens 2 (OBJ2) and a polarizing beam splitter (PBS). The probe light induces an electric field whose angular frequency ω_L is the same as that of the probe light [35], and its polarization is horizontal.

This elastically scattered coherent electric field is detected at the photo-detectors (PD1 and PD2) using the heterodyne method with the LO light with an angular frequency $\omega_L + \delta$ with δ within the squeezed bandwidth. A squeezed vacuum light beam having spectral components around the same angular frequency as the LO is focused to the same lattice site through an objective lens 1 (OBJ1). The ω_L and $\omega_L + 2\delta$ components of the squeezed vacuum reduce the shot noise in the detection around the frequency δ at the spectrum analyzer. Because the noise reduction requires exactly the same detuning and polarization as that of the signal light, the squeezed vacuum light cannot be separated from the scattered light and therefore a confocal configuration is inevitable. These three light beams are split by a half beam splitter (HBS) and then fall on two photo diodes PD1 and PD2 followed by signal subtraction via a differential amplifier.

The derivation of the R_{SN} in our scheme is discussed in detail in [appendix](#), where we assume no squeezed vacuum loss. However, the finite loss caused by real optical components as well as the imperfect spatial mode-matching between the LO and the squeezed vacuum degrade the effective squeezing level. Moreover, the imperfect spatial overlap between the LO field with a Gaussian spatial profile and the scattered light field whose spatial distribution is given as $J_1(r/\sigma)/(r/\sigma)$ also affects the R_{SN} in a similar manner as that of the probe and scattered light field in the Faraday signal (equation (5)). Consideration of the effect of loss and the spatial mode matching [36] leads to the following expression:

$$R_{SN} = \sqrt{\frac{\Gamma\tau}{2}} \eta \frac{C_{sc,LO}}{\sqrt{1 - (1 - e^{-2\xi})TC_{sv,LO}^2}}, \quad (9)$$

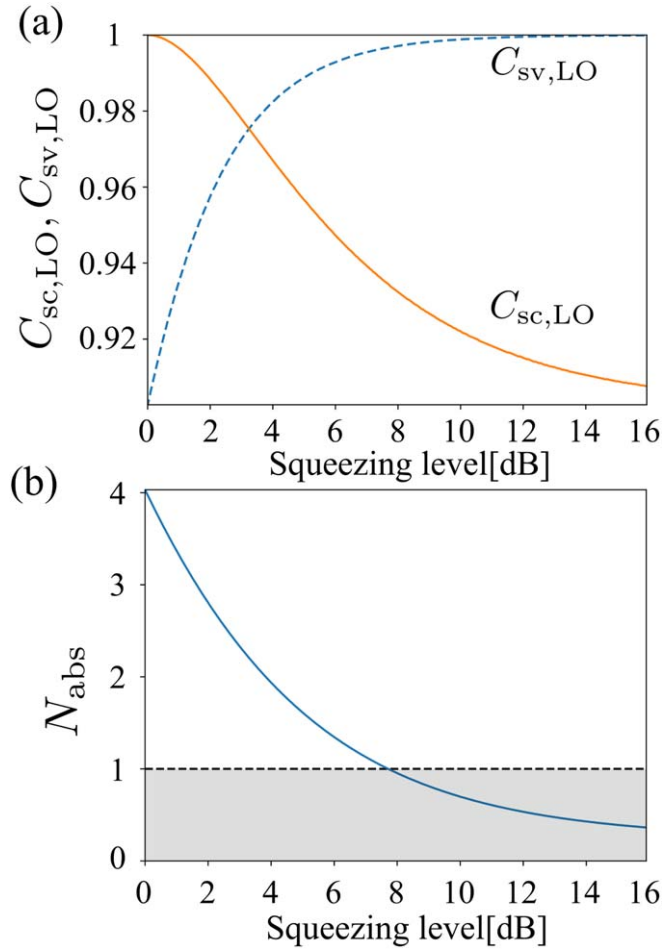


Figure 4. (a) Optimal values of $C_{sc,LO}$ and $C_{sv,LO}$ in the maximization of the R_{SN} via adjusting the LO field spatial mode. The optimal spatial mode of the local oscillator changes as the squeezing level changes. (b) Number of photon absorption events N_{abs} to maintain the R_{SN} equal to 1 plotted as a function of squeezing level. Conditions of $A_N = 0.8$, $T = 0.95$, and the optimal local oscillator light spatial mode are assumed.

where

$$C_{sv,LO} = \int_{\text{det}} \vec{E}_{sv} \cdot \vec{E}_{LO} dA / \sqrt{\int |E_{sv}|^2 dA} \sqrt{\int |E_{LO}|^2 dA} \quad (10)$$

is the level of the spatial mode-matching between the squeezed vacuum and LO, ξ is the effective squeezing parameter, and T is the transmittance of the squeezed vacuum in the detection setup. Note that in the expression of $C_{sc,LO}$, E_{probe} in equation (5) is replaced with E_{LO} . In the following calculation we again assume a Gaussian mode for the squeezed vacuum. The optimization of the LO light spatial mode results in the following expression of the optimized R_{SN}

$$(R_{SN})_{\text{opt}} = \sqrt{N_{abs}\eta} \sqrt{1 + C_{sc,sv}^2 \frac{T(1 - e^{-2\xi})}{1 - T(1 - e^{-2\xi})}}. \quad (11)$$

This indicates that the mode-matching dependence of the R_{SN} is finally characterized by

$$C_{sc,sv} = \int \vec{E}_{sv} \cdot \vec{E}_{sc} dA / \sqrt{\int |E_{sv}|^2 dA} \sqrt{\int |E_{sc}|^2 dA}, \quad (12)$$

which represents the level of the spatial overlap between the squeezed vacuum and scattered light field. Note that the optimal spatial mode of the local oscillator changes as the squeezing level changes, as shown in figure 4(a). By taking the maximum value of 0.9 for $C_{sc,sv}$ and setting the $(R_{SN})_{\text{opt}} = 1$ in equation (11), we obtain the number of photon absorption events N_{abs} to maintain the R_{SN} equal to 1 as a function of the squeezing level. Figure 4(b) shows the results with the realistic condition of $A_N = 0.8$ and $T = 0.95$. The calculated squeezing level required to achieve nondestructive detection indicated by the shaded area in the figure ($N_{abs} < 1$) is 7.7 dB, which corresponds to average photon number of 1.0.

4. Feasibility

The feasibility of the proposed scheme is discussed by considering an example of ultracold two-electron atoms in a metastable state. While the transition from the ground states of alkali atoms or two-electron atoms mostly lies in the visible region, a higher level of squeezing has been realized in the near-infrared region [37]. Notably, the transitions from the metastable states of two-electron atoms have optical transitions in the near-infrared region; for example, a Yb atom has an electric-dipole allowed transition between the 3P_0 and 3D_1 states with a corresponding wavelength of $\lambda = 1389$ nm. The transitions associated with the 3P_0 state can be used for probing a $SU(N)$ symmetric Fermi Hubbard model realized in the metastable 3P_0 state for fermionic isotopes of Yb atoms. A glass-cell system with an effective numerical aperture A_N of 0.7 of two objective lenses on both sides similar to our scheme is commercially available. Assuming 15 dB of squeezing and 95% transmittance of the optical system ($T = 0.95$) with $A_N = 0.8$ and $C_{sc,sv} = 0.9$, we expect the relation

$$N_{\text{abs}} = 0.39 \times R_{\text{SN}}^2, \quad (13)$$

which implies nondestructive detection of a single atom in a single site. As a typical experimental condition, we consider a probe beam with a pulse width of $\tau = 10 \mu\text{s}$, intensity of $I_0/I_{\text{sat}} = 1.0 \times 10^3$, and detuning of $\delta_B/\Gamma = 100$. With these parameters, the number of absorbed photons can be estimated to be $N_{\text{abs}} = 0.39$ from equation (7) and the signal-to-noise ratio $R_{\text{SN}} = 1.0$ from equation (11), consistent with equation (13), thus realizing nondestructive imaging for a single atom in a single site. The measurement time of $\tau = 10 \mu\text{s}$ is sufficiently short to perform repetitive measurements for many sites in a scanning manner in a relatively shallow lattice. In fact, for example, when we consider 15 atoms in an optical lattice with a depth of $10 \hbar\omega_R$, where the tunneling time $\tau_{\text{hop}} = \hbar/J$ is 8 ms for the lattice constant of 532 nm with J being the hopping energy, we can perform $N = 15$ measurements in $15\tau = 0.15$ ms, during which the number of hopping to adjacent sites for all 15 atoms $N_{\text{hop}} = 15 \times 0.15\text{ms}/\tau_{\text{hop}}$ is 0.28. Note that the excitation of the atoms caused by the 15 dB squeezed vacuum is negligible because of the weak intensity comparable to I_{sat} and the squeezed bandwidth is assumed to be sufficiently broad to cover the heterodyne frequency of $\delta/(2\pi) = 1$ MHz.

The above-mentioned feasibility of the scheme using a squeezed vacuum is still limited when we consider the usefulness on the many-body level such as 15 atoms. However, by combining the two proposed approaches in this work, we can provide the route to a high-fidelity nondestructive measurement on the many-body level. Namely, we consider the scheme in which we perform a probing with a squeezed vacuum, described in the second part of the section 3, for atoms without internal-degrees of freedom in the ground state trapped in an optical lattice with a magic-wavelength condition for the probe transition, as described in the first part of the section 3. Then the nondestructive condition is relaxed by $4 \times \zeta^2$ where the additional contribution ζ^2 comes from the excitation with a blue sideband in the present off-resonant-excitation scheme, different from the resonant-excitation scheme considered in the section 3. Since the condition of $\zeta = 0.11$ is already realized [31], we can improve the performance up to $R_{\text{SN}} = 25$ with a probability of changing the vibrational state of $p = 0.39$ for a single atom. In other words, with the condition of $R_{\text{SN}} = 1$, p will be 1.6×10^{-2} , and therefore the change of the vibrational state is negligible. On the many-body level of 15 atoms, this means that less than one photon is scattered for detecting 15 atoms nondestructively about the vibrational state.

5. Conclusion

In conclusion, we have proposed a quantum gas microscope capable of nondestructive detection of a single atom enabling a number of fascinating research inquiries. We derive the general relation between the R_{SN} and photon absorption of a probe beam for dispersive Faraday quantum gas microscopy and show that the detection of the atom with the R_{SN} greater than unity should be accompanied by the absorption of the probe beam by more than one photon. For an atom that has an electronic ground state without spin degrees of freedom, we find that the magic-wavelength condition of the optical lattice for the transition for probing enables detection of an atom with avoidance of excitations to higher-band. We also consider a more general scheme to detect an atom with an absorption of less than one photon based on a squeezed vacuum in a scanning microscope configuration. An application to ultracold two-electron atoms is also discussed. The combined scheme of the proposed two approaches enables a nondestructive measurement on the many-body level of about 15 atoms.

Acknowledgments

This work was supported by the Grant-in-Aid for Scientific Research of the Ministry of Education, Culture Sports, Science, and Technology/Japan Society for the Promotion of Science (MEXT/JSPS KAKENHI) Nos. 25220711 and 17H06138, 18H05405, and 18H05228; the Impulsing Paradigm Change through Disruptive Technologies (ImPACT) program; Japan Science and Technology Agency CREST (No. JPMJCR1673), and MEXT Quantum Leap Flagship Program (MEXT Q-LEAP) Grant Number JPMXS0118069021.

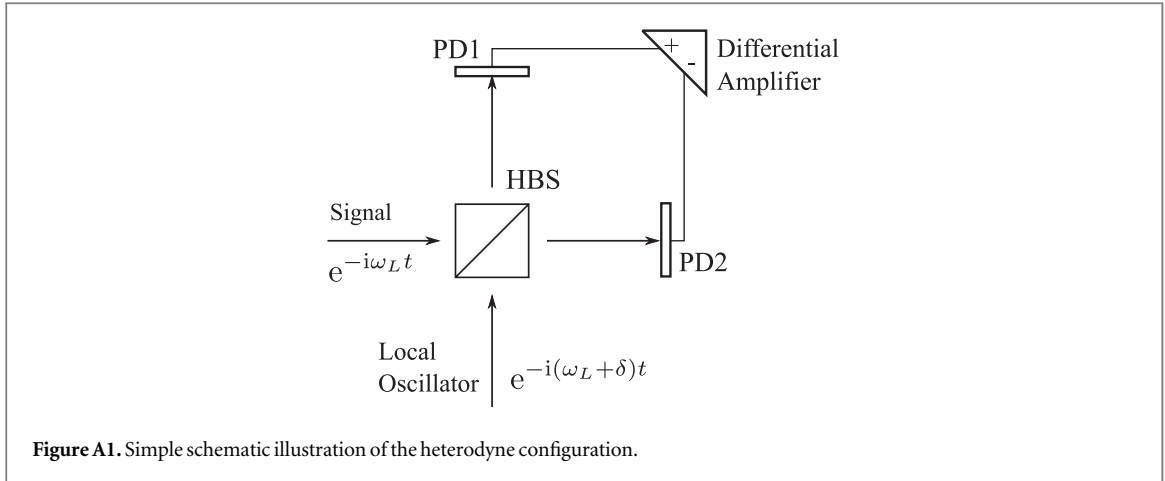


Figure A1. Simple schematic illustration of the heterodyne configuration.

Appendix. Derivation of the signal-to-noise ratio in the Heterodyne detection

An incidence of an electromagnetic field \vec{E} on a photo diode with a detection efficiency η_0 yields a photocurrent given by

$$I = \eta_0 e \int_{\text{det}} \left(\frac{\epsilon_0 c}{2} \right) |\vec{E}|^2 dA \frac{\lambda}{hc}, \quad (\text{A.1})$$

where the field intensity is integrated over the area A of the detector. The number of corresponding photoelectrons emitted during the exposure time τ is $N_e = I\tau/e$. If each detection event obeys Poisson statistics, the fluctuation of the photoelectrons $\langle \Delta N_e^2 \rangle$ is equal to its mean value $\langle N_e \rangle$. This results in the current shot noise within the frequency interval ν and $\nu + \Delta \nu$ described by $\langle i_N^2(\nu) \rangle = 2e\bar{I}\Delta\nu$, where \bar{I} is the average current. The detection bandwidth $\Delta\nu$ is related to the exposure time τ such that $2\Delta\nu = 1/\tau$.

In the heterodyne detection (figure A1), two following electric fields from the HBS are measured at the photo diodes (PD1 and PD2):

$$\vec{E}_1 = \frac{1}{\sqrt{2}} (\vec{E}_{\text{sig}} e^{-i\omega_L t} + \vec{E}_{\text{LO}} e^{-i(\omega_L + \delta)t}), \quad (\text{A.2})$$

$$\vec{E}_2 = \frac{1}{\sqrt{2}} (\vec{E}_{\text{sig}} e^{-i\omega_L t} - \vec{E}_{\text{LO}} e^{-i(\omega_L + \delta)t}). \quad (\text{A.3})$$

Each photo diode generates photocurrent I_1 and I_2 similar to equation (A.1) as well as photoelectrons. These two currents are subtracted, and the balanced current gives the signal

$$I_1 - I_2 = \eta_0 e \int_{\text{det}} \left(\frac{\epsilon_0 c}{2} \right) (\vec{E}_{\text{sig}}^* \cdot \vec{E}_{\text{LO}} e^{-i\delta t} + \vec{E}_{\text{sig}} \cdot \vec{E}_{\text{LO}}^* e^{+i\delta t}) dA \frac{\lambda}{hc}. \quad (\text{A.4})$$

We measure the δ angular frequency component, such that the signal current is obtained as follows:

$$I_S = \eta_0 e \int_{\text{det}} \left(\frac{\epsilon_0 c}{2} \right) \vec{E}_{\text{sig}}^* \cdot \vec{E}_{\text{LO}} dA \frac{\lambda}{hc}, \quad (\text{A.5})$$

and the number of corresponding photoelectrons is $N_S = I_S \tau / e$. If the LO intensity is sufficiently strong, i.e. $|\vec{E}_{\text{LO}}|^2 \gg |\vec{E}_{\text{sig}}|^2$, its shot noise is dominant and given by the following:

$$\langle i_S^2(\nu) \rangle = 2\eta_0 e^2 \int_{\text{det}} \left(\frac{\epsilon_0 c}{2} \right) |\vec{E}_{\text{LO}}|^2 dA \frac{\lambda}{hc} \Delta\nu \equiv \Phi_0 \Delta\nu, \quad (\text{A.6})$$

where \vec{E}_{LO} is the average amplitude of the LO field and $\omega_L = 2\pi\nu \gg \delta$ is assumed. The corresponding fluctuation of the photoelectrons emitted is $\langle \Delta N_S^2 \rangle = \Phi_0 \tau / 2e^2$. The square root of this quantity corresponds to the noise in equation (3) by assuming a perfect detector ($\eta_0 = 1$) and using the relation $2\Delta\nu = 1/\tau$.

Accordingly, the ratio $N_S / \sqrt{\langle \Delta N_S^2 \rangle}$ yields a signal-to-noise ratio R_{SN} in equation (2) in which the subscripts 'sig' and 'LO' are replaced by 'sc' and 'probe,' respectively.

A squeezed vacuum state of light is used to reduce the detection noise and fed into the signal port. The squeezed vacuum can be generated by a subthreshold degenerate optical parametric oscillator (OPO) [37]. The output spectrum for the squeezed quadrature variance is given by the following [38]

$$S(\nu) = -\frac{4\sqrt{P/P_{\text{th}}}}{(2\pi\nu/\gamma)^2 + (1 + \sqrt{P/P_{\text{th}}})^2}, \quad (\text{A.7})$$

where P is the pump power for the OPO with the oscillation threshold P_{th} and γ is the OPO-cavity linewidth. The measured current fluctuation is calculated as follows:

$$\langle i_M^2(\nu) \rangle = \Phi_0[1 + \eta_{\text{tot}}S(\nu)]\Delta\nu, \quad (\text{A.8})$$

where η_{tot} is the total detection efficiency. Accordingly, we can define the effective squeezing parameter $\xi(\nu)$ for the sideband frequency component and also the corresponding signal-to-noise ratio, which are addressed in the discussion in the main text.

ORCID iDs

Katsunari Enomoto  <https://orcid.org/0000-0002-4980-4216>

Nobuyuki Takei  <https://orcid.org/0000-0002-0720-3033>

References

- [1] Bakr W S, Gillen J I, Peng A, Fölling S and Greiner M 2009 *Nature* **462** 74
- [2] Sherson J F, Weitenberg C, Endres M, Cheneau M, Bloch I and Kuhr S 2010 *Nature* **467** 68
- [3] Haller E, Hudson J, Kelly A, Cotta D A, Peaudecerf B, Bruce G D and Kuhr S 2015 *Nat. Phys.* **11** 738
- [4] Cheuk L W, Nichols M A, Okan M, Gersdorf T, Ramasesh V V, Bakr W S, Lompe T and Zwierlein M W 2015 *Phys. Rev. Lett.* **114** 193001
- [5] Omran A, Boll M, Hilker T A, Kleinlein K, Salomon G, Bloch I and Gross C 2015 *Phys. Rev. Lett.* **115** 263001
- [6] Parsons M F, Huber F, Mazurenko A, Chiu C S, Setiawan W, Wooley-Brown K, Blatt S and Greiner M 2015 *Phys. Rev. Lett.* **114** 213002
- [7] Edge G J A, Anderson R, Jervis D, McKay D C, Day R, Trotzky S and Thywissen J H 2015 *Phys. Rev. A* **92** 063406
- [8] Weitenberg C, Endres M, Sherson J F, Cheneau M, Schauß P, Fukuhara T, Bloch I and Kuhr S 2011 *Nature* **471** 319
- [9] Gross C and Bloch I 2017 *Science* **357** 6355
- [10] Preiss P M, Ma R, Tai M E, Lukin A, Rispoli M, Zupancic P, Lahini Y, Islam R and Greiner M 2015 *Science* **347** 1229
- [11] Parsons M F, Mazurenko A, Chiu C S, Ji G, Greif D and Greiner M 2016 *Science* **353** 1253
- [12] Boll M, Hilker T A, Salomon G, Omran A, Nespolo J, Pollet L, Bloch I and Gross C 2016 *Science* **353** 6305
- [13] Cheuk L W, Nichols M A, Lawrence K R, Okan M, Zhang H, Khatami E, Trivedi N, Paiva T, Rigol M and Zwierlein M W 2016 *Science* **353** 1260
- [14] Islam R, Ma R, Preiss P M, Tai M E, Lukin A, Rispoli M and Greiner M 2015 *Nature* **528** 77
- [15] Ozawa M 2004 *Ann. Phys.* **311** 350
- [16] Ashida Y and Ueda M 2017 *Phys. Rev. A* **95** 022124
- [17] Mazzucchi G, Caballero-Benitez S F, Ivanov D A and Mekhov I B 2016 *Optica* **3** 1213
- [18] Yang D, Laflamme C, Vasilyev D V, Baranov M A and Zoller P 2018 *Phys. Rev. Lett.* **120** 133601
- [19] Yang D, Vasilyev D V, Laflamme C, Baranov M A and Zoller P 2018 *Phys. Rev. A* **98** 023852
- [20] Lye J E, Hope J J and Close J D 2003 *Phys. Rev. A* **67** 043609
- [21] Hope J J and Close J D 2004 *Phys. Rev. Lett.* **93** 180402
- [22] Hope J J and Close J D 2005 *Phys. Rev. A* **71** 043822
- [23] Andersen U L, Gehring T, Marquardt C and Leuchs G 2016 *Phys. Scr.* **91** 053001
- [24] Wolfgang F, Cerè A, Beduini F A, Predojević A, Koschorreck M and Mitchell M W 2010 *Phys. Rev. Lett.* **105** 053601
- [25] Otterstrom N, Pooser R C and Lawrie B J 2014 *Opt. Lett.* **39** 6533
- [26] Polzik E S, Carri J and Kimble H J 1992 *Phys. Rev. Lett.* **68** 3020
- [27] Yamamoto R, Kobayashi J, Kato K, Kuno T, Sakura Y and Takahashi Y 2017 *Phys. Rev. A* **96** 033610
- [28] Novotny L and Hecht B 2012 *Principles of Nano-Optics* (Cambridge: Cambridge University Press)
- [29] Tey M K, Maslennikov G, Liew T C H, Aljunid S A, Huber F, Chng B, Chen Z, Scarani V and Kurtsiefer C 2009 *New J. Phys.* **11** 043011
- [30] Wineland D J, Itano W M, Bergquist J C and Hulet R G 1987 *Phys. Rev. A* **36** 2220
- [31] Yamamoto R, Kobayashi J, Kuno T, Kato K and Takahashi Y 2016 *New J. Phys.* **18** 031001
- [32] Grote H, Danzmann K, Dooley K L, Schnabel R, Slutsky J and Vahlbruch H 2013 *Phys. Rev. Lett.* **110** 181101
- [33] Taylor M A, Janousek J, Daria V, Knittel J, Hage B, Bachor H-A and Bowen W P 2013 *Nat. Photon.* **7** 229
- [34] Braunstein S L and van Loock P 2005 *Rev. Mod. Phys.* **77** 513
- [35] Loudon R 2000 *The Quantum Theory of Light* (Oxford: Oxford University Press)
- [36] Bennink R S and Boyd R W 2002 *Phys. Rev. A* **66** 053815
- [37] Vahlbruch H, Mehmet M, Danzmann K and Schnabel R 2016 *Phys. Rev. Lett.* **117** 110801
- [38] Polzik E S, Carri J and Kimble H J 1992 *Appl. Phys. B* **55** 279